GENERALIZED FORM FACTORS FOR THE BEAM COUPLING IMPEDANCES IN A FLAT CHAMBER

N. Mounet (EPFL, Lausanne and CERN, Geneva) and E. Métral (CERN, Geneva)

Abstract

The exact formalism from B. Zotter to compute beam coupling impedances has been fully developed only in the case of an infinitely long circular beam pipe. For other two dimensional geometries, some form factors are known only in the ultrarelativistic case and under certain assumptions of conductivity and frequency of the pipe material. We present here a new and exact formalism to compute the beam coupling impedances in the case of a collimator-like geometry where the jaws are made of two infinite plates of any linear material. It is shown that the impedances can be computed theoretically without any assumptions on the beam speed, material conductivity or frequency range. The final formula involves coefficients in the form of integrals that can be calculated numerically. This way we obtain new generalized form factors between the circular and the flat chamber cases, which eventually reduce to the so-called Yokoya factors under certain conditions.

INTRODUCTION

Recently, it has been shown that the usual approach to compute the beam coupling impedances of a flat chamber, i.e. thanks to a formula valid for an axisymmetric geometry [1] multiplied by constant "Yokoya" factors [2, 3], fails in the case of non metallic materials such as ferrite [4]. Indeed, the hypotheses on which the Yokoya factors theory relies (in particular on the conductivity and skin depth of the material) turn out to be wrong for certain materials.
To provide a more general theory on the flat chamber impedance, we use similar ideas as the original Zotter's formalism for a cylindrical pipe [5] and apply them to an infinitely long, thick and large flat chamber. Details on the derivations below will be shown in a later publication [6].

ELECTROMAGNETIC CONFIGURATION

We consider a point-like beam of charge Q travelling at a speed $v = \beta c$ along an infinitely long and large flat chamber of half gap b. The beam is at the position $(x = 0, y = y_1, s = vt)$ in cartesian coordinates. The source charge density is in frequency domain ($f = \frac{\omega}{2\pi}$) [7]

$$\rho(x, y, s; \omega) = \frac{Q}{v}\delta(x)\delta(y - y_1)e^{-jks}, \qquad (1)$$

where $k \equiv \frac{\omega}{v}$ and δ is the Dirac distribution. Using the horizontal Fourier transform and dropping the $\int_0^{+\infty} \mathrm{d}k_x$ factor, we want first to compute the response to the source

$$\tilde{\rho}(k_x, y, s; \omega) = \frac{Q}{\pi v}\cos(k_x x)\delta(y - y_1)e^{-jks}, \qquad (2)$$

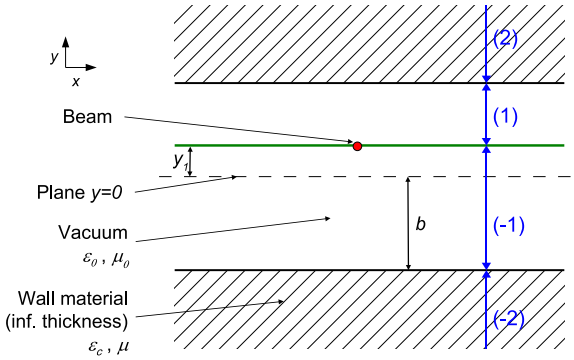

Figure 1: Cross section of the flat chamber.

which corresponds to a surface charge density on the plane $y = y_1$. The space is therefore divided into 4 layers parallel to the $y = 0$ plane (see Fig. 1), denoted by the superscript (p) where $p = -2, -1, 1$ or 2. The inner layers are vacuum while the outer ones are made of a single, linear, homogeneous and isotropic medium.
The macroscopic Maxwell equations in frequency domain for the electric and magnetic fields $\vec{E}$ and $\vec{H}$ are written [5]

$$\vec{\mathrm{curl}}\vec{H} - j\omega\vec{D} = \tilde{\rho}v\vec{e_s}, \quad \vec{\mathrm{curl}}\vec{E} + j\omega\vec{B} = 0,$$
$$\mathrm{div}\vec{D} = \tilde{\rho}, \ \mathrm{div}\vec{B} = 0, \quad \vec{D} = \varepsilon_c\vec{E}, \ \vec{B} = \mu\vec{H},$$

where [8]

$$\varepsilon_c = \varepsilon_0\varepsilon_1 = \varepsilon_0\varepsilon_b\left[1 - j\tan\vartheta_E\right] + \frac{\sigma_{DC}}{j\omega\left(1 + j\omega\tau\right)}, \qquad (3)$$
$$\mu = \mu_0\mu_1 = \mu_0\mu_r\left[1 - j\tan\vartheta_M\right]. \qquad (4)$$

In these expressions, ε_0 (μ_0) is the permittivity (permeability) of vacuum, ε_b the real dielectric constant, μ_r the real part of the relative complex permeability, $\tan\vartheta_E$ ($\tan\vartheta_M$) the dielectric (magnetic) loss tangent, σ_{DC} the DC conductivity and τ the relaxation time. We use the Drude model [9, p. 312] for the AC conductivity, and assume the validity of local Ohm's law.

ELECTROMAGNETIC FIELDS

From Maxwell equations, one can get

$$\left[\frac{\partial^2}{\partial x^2} + \frac{\partial^2}{\partial y^2} + \frac{\partial^2}{\partial s^2} + \omega^2\varepsilon_c\mu\right]E_s = \frac{1}{\varepsilon_c}\frac{\partial\tilde{\rho}}{\partial s} + j\omega\mu\tilde{\rho}v, \qquad (5)$$

$$\left[\frac{\partial^2}{\partial x^2} + \frac{\partial^2}{\partial y^2} + \frac{\partial^2}{\partial s^2} + \omega^2\varepsilon_c\mu\right]H_s = 0. \qquad (6)$$

Solutions are sought in the form $X(x)Y(y)S(s)$. We get three harmonic differential equations, and from the finiteness of $X(\pm\infty)$ and the symmetries of the problem:

$$X_{E_s}(x) \propto \cos(k_{x_e}x), \qquad X_{H_s}(x) \propto \sin(k_{x_h}x),$$
$$S_{E_s}(s) \propto e^{-jks}, \qquad S_{H_s}(s) \propto e^{-jks}.$$

From the boundary conditions at $y = \pm b$ and $y = y_1$ it can be shown that $k_{x_e} = k_{x_h} = k_x$ in all the layers. Defining then $\nu^{(p)} \equiv k\sqrt{1-\beta^2\varepsilon_1^{(p)}\mu_1^{(p)}}$ and $k_y^{(p)} = \sqrt{k_x^2+{\nu^{(p)}}^2}$, we get the fields longitudinal components in layer (p):

$$E_s^{(p)} = \cos(k_x x)e^{-jks}\left[C_{e+}^{(p)}e^{k_y^{(p)}y} + C_{e-}^{(p)}e^{-k_y^{(p)}y}\right], \quad (7)$$

$$H_s^{(p)} = \sin(k_x x)e^{-jks}\left[C_{h+}^{(p)}e^{k_y^{(p)}y} + C_{h-}^{(p)}e^{-k_y^{(p)}y}\right], \quad (8)$$

where the constants $C_{e+}^{(p)}$, $C_{e-}^{(p)}$, $C_{h+}^{(p)}$ and $C_{h-}^{(p)}$ depend on k_x and ω. The transverse components are found from

$$E_x^{(p)} = \frac{jk}{{\nu^{(p)}}^2}\left(\frac{\partial E_s^{(p)}}{\partial x} + \upsilon\mu^{(p)}\frac{\partial H_s^{(p)}}{\partial y}\right), \quad (9)$$

$$E_y^{(p)} = \frac{jk}{{\nu^{(p)}}^2}\left(\frac{\partial E_s^{(p)}}{\partial y} - \upsilon\mu^{(p)}\frac{\partial H_s^{(p)}}{\partial x}\right), \quad (10)$$

$$H_x^{(p)} = \frac{jk}{{\nu^{(p)}}^2}\left(-\upsilon\varepsilon_c^{(p)}\frac{\partial E_s^{(p)}}{\partial y} + \frac{\partial H_s^{(p)}}{\partial x}\right), \quad (11)$$

$$H_y^{(p)} = \frac{jk}{{\nu^{(p)}}^2}\left(\upsilon\varepsilon_c^{(p)}\frac{\partial E_s^{(p)}}{\partial x} + \frac{\partial H_s^{(p)}}{\partial y}\right). \quad (12)$$

Then the boundary conditions at $y = y_1$ give

$$C_{e+}^{(1)} = C_{e+}^{(-1)} - \mathcal{C}\frac{e^{-k_y^{(1)}y_1}}{k_y^{(1)}}, \quad C_{e-}^{(1)} = C_{e-}^{(-1)} + \mathcal{C}\frac{e^{k_y^{(1)}y_1}}{k_y^{(1)}},$$

with $\mathcal{C} = \frac{j\omega\mu_0 Q}{2\pi\beta^2\gamma^2}$ and $\gamma^2 = \frac{1}{1-\beta^2}$. The finiteness of $Y(\pm\infty)$ reduce the number of unknowns to 8, while the boundary conditions at $y = \pm b$ provide 8 distinct equations which can be solved analytically [6]. Noticing that in the vacuum region $\nu^{(\pm1)} = \frac{k}{\gamma}$, while in the chamber material we can drop the superscript (±2) for ν, μ and ε_c, such that $k_y^{(\pm1)} = \sqrt{k_x^2+\frac{k^2}{\gamma^2}}$ and $k_y^{(\pm2)} = \sqrt{k_x^2+\nu^2}$, we obtain:

$$C_{e+}^{(1)} = -\frac{\mathcal{C}}{k_y^{(1)}}\left[\chi(k_x)e^{k_y^{(1)}y_1} + \eta(k_x)e^{-k_y^{(1)}y_1}\right], \quad (13)$$

$$C_{e-}^{(-1)} = -\frac{\mathcal{C}}{k_y^{(1)}}\left[\eta(k_x)e^{k_y^{(1)}y_1} + \chi(k_x)e^{-k_y^{(1)}y_1}\right], \quad (14)$$

with

$$\chi(k_x) = \frac{g_6g_3 - g_2g_7}{g_1g_6 - g_2g_5}, \qquad \eta(k_x) = \frac{g_6g_4 - g_2g_8}{g_1g_6 - g_2g_5},$$

$$g_1 = e^{-k_y^{(1)}b}\left(-f_5^2f_1 + f_2^2f_3\right) + e^{3k_y^{(1)}b}f_1\left(f_5^2 - f_1f_3\right),$$
$$g_2 = e^{k_y^{(1)}b}\left(f_5^2f_2 - f_1^2f_4\right) + e^{-3k_y^{(1)}b}f_2\left(f_2f_4 - f_5^2\right),$$
$$g_3 = e^{k_y^{(1)}b}f_1\left(f_5^2 - f_1f_4\right) + e^{-3k_y^{(1)}b}f_2\left(f_2f_4 - f_5^2\right),$$
$$g_4 = e^{-k_y^{(1)}b}f_5^2\left(f_2 - f_1\right),$$
$$g_5 = e^{-k_y^{(1)}b}\left(f_4(f_1 - f_2) - f_2f_3 + f_5^2\right) + e^{3k_y^{(1)}b}\left(-f_5^2 + f_1f_3\right),$$
$$g_6 = e^{k_y^{(1)}b}\left(f_3(f_1 - f_2) - f_5^2 + f_1f_4\right) + e^{-3k_y^{(1)}b}\left(-f_2f_4 + f_5^2\right),$$
$$g_7 = e^{k_y^{(1)}b}\left(-f_5^2 + f_1f_4\right) + e^{-3k_y^{(1)}b}\left(-f_2f_4 + f_5^2\right),$$
$$g_8 = e^{-k_y^{(1)}b}f_4\left(f_1 - f_2\right),$$

and

$$f_{1,2} = \upsilon\left(\pm\frac{\gamma^2\mu_0}{k^2}k_y^{(1)} + \frac{\mu}{\nu^2}k_y^{(2)}\right),$$
$$f_{3,4} = \upsilon\left(\pm\frac{\gamma^2\varepsilon_0}{k^2}k_y^{(1)} + \frac{\varepsilon_c}{\nu^2}k_y^{(2)}\right), f_5 = k_x\left(\frac{\gamma^2}{k^2} - \frac{1}{\nu^2}\right).$$

Note that χ and η depend on k_x but not on y_1. The total fields due to our initial point-like source are obtained by integration over k_x. Using the polar coordinates (r,θ) in the (x,y) plane, we can obtain E_s in vacuum [6]:

$$E_{s,tot}^{vac} = \mathcal{C}e^{-jks}\left[K_0\left(\frac{k}{\gamma}\sqrt{x^2+(y-y_1)^2}\right)\right.$$
$$\left. -4\sum_{m,n=0}^{+\infty}\frac{\alpha_{mn}\cos\left(n\theta - \frac{n\pi}{2}\right)}{(1+\delta_{m0})(1+\delta_{n0})}I_m\left(\frac{ky_1}{\gamma}\right)I_n\left(\frac{kr}{\gamma}\right)\right], \quad (15)$$

where $\delta_{i0} = 1$ if $i = 0$, 0 otherwise, and α_{mn} are obtained by integrals that can be computed numerically:

$$\alpha_{mn} = \left\{(-1)^{m+n}+1\right\}\int_0^{+\infty}\mathrm{d}v\,(\cosh mv)\,(\cosh nv)$$
$$\left[\chi\left(\frac{k}{\gamma}\sinh v\right) + (-1)^m\eta\left(\frac{k}{\gamma}\sinh v\right)\right]. \quad (16)$$

The first term in $E_{s,tot}^{vac}$ is the direct space-charge part, which is the same as the one found for a cylindrical geometry [10]. The other term is the "wall" part of the fields, as α_{mn} depend only on the chamber properties and on ω.

IMPEDANCES AND FORM FACTORS

We can now proceed to the impedances (longitudinal and transverse) for a test particle located at (x_2, y_2), and generalizing the source position at (x_1, y_1). We use the definitions from [1] and Eqs. (9) to (12) in vacuum:

$$Z_\parallel = -\frac{1}{Q}\int\mathrm{d}sE_{s,tot}^{vac}(x_2,y_2,s;\omega)e^{jks}, \quad (17)$$

$$Z_x = -\frac{1}{kQ}\int\mathrm{d}s\frac{\partial E_{s,tot}^{vac}}{\partial x}(x_2,y_2,s;\omega)e^{jks}, \quad (18)$$

$$Z_y = -\frac{1}{kQ}\int\mathrm{d}s\frac{\partial E_{s,tot}^{vac}}{\partial y}(x_2,y_2,s;\omega)e^{jks}. \quad (19)$$

The direct space-charge part of $E_{s,tot}^{vac}$ gives exactly the same multimode direct space-charge impedances as in [10].

For the wall impedances [8], restricting ourselves to the first linear terms with respect to the source and test coordinates, we get (L is the length of the element and $Z_0 = \mu_0 c$):

$$Z_{\parallel}^{Wall} = \frac{jL\mu_0\omega}{2\pi\beta^2\gamma^2}\alpha_{00}, \tag{20}$$

$$Z_x^{Wall} = \frac{jLZ_0k^2}{4\pi\beta\gamma^4}\left(\alpha_{02}-\alpha_{00}\right)\left(x_1-x_2\right), \tag{21}$$

$$Z_y^{Wall} = \frac{jLZ_0k^2}{4\pi\beta\gamma^4}\left[2\alpha_{11}y_1+\left(\alpha_{00}+\alpha_{02}\right)y_2\right]. \tag{22}$$

In the transverse impedances, the term proportional to x_1 or y_1 is the dipolar term while the one proportional to x_2 or y_2 is the quadrupolar one. Comparing the above to the formulae in [10] we get then the form factors:

$$F_{\parallel} = \frac{\alpha_{00}}{\alpha_{\mathrm{TM}}(m=0)}, \tag{23}$$

$$F_x^{dip} = \frac{\alpha_{02}-\alpha_{00}}{\alpha_{\mathrm{TM}}(m=1)},\ F_y^{dip} = \frac{2\alpha_{11}}{\alpha_{\mathrm{TM}}(m=1)}, \tag{24}$$

$$F_x^{quad} = \frac{\alpha_{00}-\alpha_{02}}{\alpha_{\mathrm{TM}}(m=1)},\ F_y^{quad} = \frac{\alpha_{00}+\alpha_{02}}{\alpha_{\mathrm{TM}}(m=1)}, \tag{25}$$

where the α_{TM} constants are for a cylindrical pipe [10].

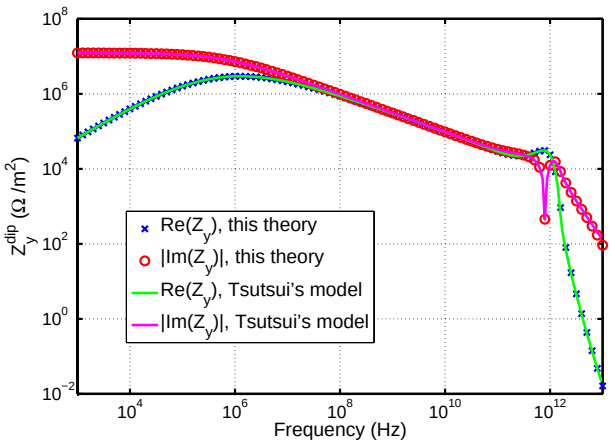

Figure 2: Vertical dipolar impedance (divided by y_1 and L) for an LHC graphite collimator ($\gamma = 479.7$, $b = 2$mm, $\mu_r = \varepsilon_b = 1$, $\vartheta_E = \vartheta_M = 0$, $\sigma_{DC} = 10^5$S/m, $\tau = 0.8$ps).

As a first check of this theory, we have plotted in Fig. 2 the vertical dipolar impedance of an LHC graphite collimator, comparing our results to those obtained with the model in [11] on a rectangular geometry, putting the plates perpendicular to the jaws 25cm apart and taking the graphite thickness as 25cm, in order to get closer to the case of an infinitely large and thick chamber. The agreement between the two approaches is very good.

We have then plotted our generalized frequency dependent form factors for the cases of graphite in Fig. 3 and of a ceramic (hBN) in Fig. 4. The form factors are complex numbers but their imaginary parts are quite small (except at very high frequencies) so we did not plot them. For graphite, deviations from the usual Yokoya factors are significant only at high frequencies. For hBN significant differences with the Yokoya factors appear at all frequencies.

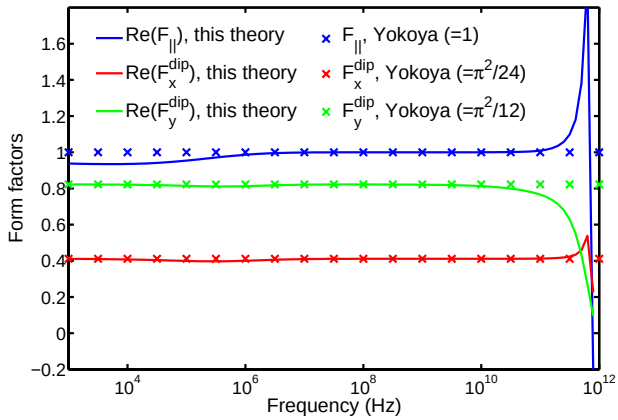

Figure 3: Form factors for graphite (parameters of Fig. 2).

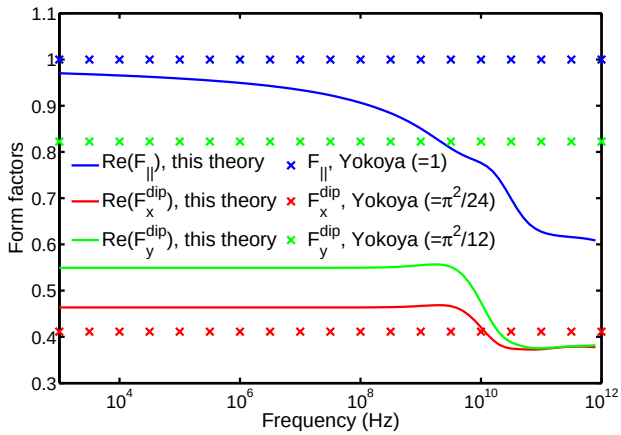

Figure 4: Form factors for an hBN ceramic ($\gamma = 479.7$, $b = 4$mm, $\mu_r = 1$, $\varepsilon_b = 2$, $\vartheta_E = \vartheta_M = \tau = 0$, $\sigma_{DC} = 0.25 \cdot 10^{-12}$S/m).

CONCLUSION

New generalized frequency dependent form factors between the flat and cylindrical chambers impedances have been obtained. As was also seen by other means for a SPS kicker [4], those form factors can be quite different from the usual constant Yokoya factors for non metallic materials. An extension of this theory to the multilayer case is foreseen.

REFERENCES

[1] E. Métral et al, PAC'07, Albuquerque, USA (2007).
[2] R. L. Gluckstern et al, Phys. Rev. E 47 (1993) 1, p. 656.
[3] K. Yokoya, Part. Acc., 41 (1993), p. 221.
[4] B. Salvant, N. Mounet, C. Zannini et al, these proceedings.
[5] B. Zotter, CERN-AB-2005-043 (2005).
[6] N. Mounet and E. Métral, CERN note, to be published.
[7] R. L. Gluckstern, CERN-2000-011 (2000).
[8] F. Roncarolo et al, Phys. Rev. ST AB 12 (2009) 084401.
[9] J. D. Jackson, "Classical Electrodynamics", 3rd ed (1998).
[10] N. Mounet and E. Métral, these proceedings.
[11] H. Tsutsui, LHC Project Note 318 (2003).